Revista Brasileira de Geofísica
RBGf
Brazilian Journal of Geophysics

Revista Brasileira de Geofísica (2015) 33(4): 1-10

ISSN 0102-261X
www.scielo.br/rbg

QUARTZ PROSPECTING WITH INDUCED POLARIZATION (IP) AND RESISTIVITY BY USING GRADIENT AND DIPOLE-DIPOLE ARRAYS

José Domingos Faraco Gallas

ABSTRACT. Geophysical surveys were accomplished in Bahia, Brazil, and they aimed at detecting resistivity and/or IP geophysical anomalies that may be correlated to large quartz mass occurrences that, in some cases, may have economic interest (hyaline high-quality quartz or quartz with rutile inclusions). These quartz masses occur in granitic rocks. The indirect geophysical detection of quartz masses was possible, however it could not differentiate the aforementioned types of quartz. After digging wells and trenches, the presence of milky quartz masses, without economic interest, was confirmed.

Keywords: resistivity, IP, quartz prospecting.

RESUMO. Os levantamentos geofísicos foram efetuados no interior da Bahia, Brasil, e tiveram como objetivo a detecção de anomalias geofísicas de resistividade e/ou IP que pudessem ser correlacionáveis às ocorrências de grandes massas quartzosas que, em alguns casos, podem conter quartzo de interesse econômico – quartzo hialino de boa qualidade ou com inclusões de rutilo. Estas massas quartzosas estão contidas em rochas de composição granítica. A detecção de massas quartzosas por meios geofísicos indiretos foi possível, contudo não permitiu diferenciar os tipos de quartzo supracitados. Conforme confirmações posteriores com escavação de poços e trincheiras, os resultados detectaram a presença das massas quartzosas, porém de quartzo leitoso, sem interesse econômico.

Palavras-chave: resistividade, IP, prospecção de quartzo.

Universidade de São Paulo – USP, Instituto de Geociências, Departamento de Geologia Sedimentar e Ambiental, Rua do Lago, 562, 05508-080 São Paulo, SP, Brazil. Phone: +55(11) 3091-4232 – E-mail: jgallas@usp.br

INTRODUCTION

The main objective of this work was to test the efficiency of electrical resistivity and induced polarization surveys, to characterize subsurface occurrences of high-quality hyaline quartz and/or quartz with rutile inclusions.

The indirect geophysical detection of quartz masses was possible, however it could not differentiate the aforementioned types of quartz. After digging wells and trenches, the presence of milky quartz masses, without economic interest, was confirmed.

The use of IP-Resistivity for sulphide prospecting and environmental studies is common in the geophysical literature, however, the application of this method to quartz prospecting, used in this study, is unprecedent.

Theoretically, quartz veins should have higher resistivity, but when hydrothermal processes occur, may also have low resistivity. Otherwise, the induced polarization (IP) response related to quartz masses is unexpected, and cannot have a defined premise of high or low chargeability.

LOCAL GEOLOGY

The study area is located in Bahia, Novo Horizonte municipality, in Chapada Diamantina region. The regional geology is represented by Paleo-Mesoproterozoic rocks of the Espinhaço Supergroup and the Archean paleoproterozoic gneiss and granitic basement rocks.

The local geology is mostly represented by pink granites, almost entirely composed of K-feldspar and quartz, without visible micas, as observed in outcrops.

The constant occurrence of this lithology in the restricted area of the geophysical surveys, approximately 350 m $\times$ 100 m, was confirmed in field inspections during the surveys.

The quartz bodies, our prospecting targets, occur within the matrix of these rocks. The soil thickness are almost always less than 2-3 m, and exceptionally reaching more than 4-5 m.

THEORETICAL CONSIDERATIONS ON USED METHODS AND TECHNIQUES

Induced Polarization (IP)

Induced polarization (IP) is an electrical phenomenon caused by ground current transmission. It is observed as an out-of-phase voltage response in terrestrial materials. As geophysical measurement, induced polarization refers to a resistive blocking action or electrical polarization in terrestrial materials, with pronounced process in pores filled with fluids in the vicinity of metallic minerals. Therefore, the more intense IP effect is observed in rocks with metallic minerals. However, the exact relation between IP response and the amount of mineralization and/or polarizable material is complex, if not impossible at all.

Under favorable conditions, the main IP method advantage is its ability in detecting metal ore presence, even in very small amounts in which IP (Sumner, 1976) identifies sulphide disseminations of around 0.5% in metallic volume.

It is also possible to differentiate several lithologies that may have IP response variety due to their mineral or ionic content (Gallas et al., 2011).

The IP technique used in this study was the time domain, whose simplified description should be: When a ΔV potential difference is established due to the ground current passage, this potential difference neither instantaneously establish nor annul when the current is emitted and cut up into successive pulses. However, it describes $\Delta V_{IP} = f(t)$ curve linking ΔVp asymptote at stationary state with zero asymptote after cutting current. This phenomenon is named “Induced Polarization” (Bertin & Loeb, 1976).

Schematically, IP phenomenon in time domain can be described as shown in Figure 1.

The amount characterizing IP phenomenon is the area under discharge curve, including asymptotic part, which tends to zero, given by:

$$IP = \int_0^\infty \Delta V_{IP} dt$$

For all practical purposes, an area under discharge curve is measured by transient voltage integration in the range of a time window, from t_1 to t_2 for instrumentation and equipment electronic design reasons. Named apparent chargeability (M), the measured amount is:

$$M_{t1,t2} = \int_{t1}^{t2} \Delta V_{IP(t)} dt$$

Usually, integrated area under the decay curve is normalized as regards primary ΔV_p voltage, where:

$$M = \frac{M_{t1,t2}}{\Delta Vp} = \frac{1}{Vp} \int_{t1}^{t2} \Delta V_{IP(t)} dt$$

The ΔVp measurement is linear and proportional to current I intensity, while M value depends on I. On the other hand, apparent chargeability (M) amplitude depends on t_1 to t_2 integration time.

The $\Delta V_{IP}(t)$ behavior depends on rock polarizability. Analogously, everything happens as if the soil had small condensers charged during current emission, and discharged after it

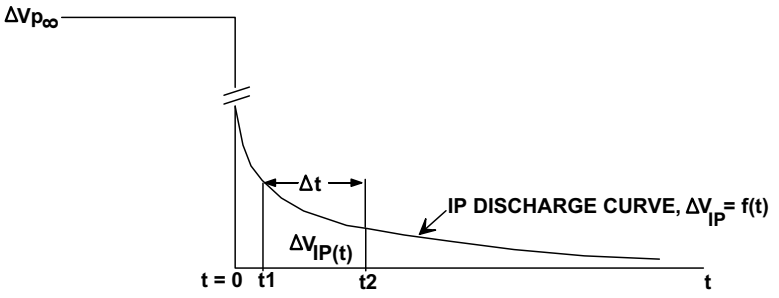

Figure 1 – IP Discharge Curve (adapted from Bertin & Loeb, 1976).

is cut off (Gallas, 2000). $\Delta V_{IP} = f(t)$ curve would be named IP discharge curve. However, this comparison is a very simplified image, because this analogy with a resistance/condenser electric circuit does not completely explain IP phenomenon.

Apparent Resistivity (ρa)

Geoelectric prospecting is one of the most important concepts in apparent resistivity. Physical data measured in an electrical resistivity field survey are the current I generated by an E source, and transmitted by two A and B electrodes. Established ΔV potential difference is measured through potential electrodes named M and N. It is possible to obtain ρ resistivity from these parameters. In a homogeneous and isotropic terrain, this resistivity is constant for any electrode dispositions used in the measurements. Figure 2 schematically illustrates electrical resistivity method.

Usually in nature, substrates are neither homogeneous nor isotropic. If the four mentioned electrodes are positioned in ρ_1, ρ_2, ρ_3 and ρ_4 resistivity sites, according Figure 3, measured resulting resistivity will not be true but a so-named ρ_a apparent resistivity ρ_a (Orellana, 1972). This will not be equal to any of the four ones but it will influence all of them, and their respective geometry.

This resistivity cannot be understood neither a mean nor weighted mean of the four resistivity. However, it could be either higher or lower than any of them (Orellana, 1972).

The apparent resistivity can be obtained from measurements accomplished in an heterogeneous medium by applying the expression valid for homogeneous media. This expression is obtained considering two current electrodes (A and B) as well as two potential measured points (M and N). The potential is considered B negative, assuming the current enters in A and exits in B.

$$\rho = \left(\frac{U_M - U_N}{I}\right) \frac{2\pi}{\frac{1}{AM} - \frac{1}{BM} - \frac{1}{AN} + \frac{1}{BN}} = K\frac{\Delta U}{I}$$

The ρ calculated values are the same ρ_a values, and they are calculated based on separation between electrodes through K geometric factor, expressed as:

$$K = \frac{2\pi}{\frac{1}{AM} - \frac{1}{BM} - \frac{1}{AN} + \frac{1}{BN}}$$

Finally, apparent resistivity can be expressed as:

$$\rho_a = K\frac{\Delta U}{I}$$

Arrays

Dipole-Dipole Array/ IP-resistivity pseudosections

Pseudosections are so called because data obtained from different investigations levels do not correspond to real parameter values of each true depth layer, and they refer to apparent IP-resistivity values. Similarly, vertical section depths are also only qualitative.

In pseudosection data interpretation, qualitative information on spatial body position in subsurface is obtained, and more rarely it can estimate its dip. As a result, the information is more accurate as the better IP-resistivity anomaly is defined.

Pseudosection electrode array used in this work was dipole-dipole. In this array, electrodes A and B of current electrodes and M/N potential or reception electrodes are aligned on the same profile. Array is defined by the spacing $\ell = AB = MN$. Research depth increases with $(n+1)l/2$ (Fig. 4).

Plotting points are attributed at 45° intersection from Ω and O each dipole origins, indicating theoretical depth reached for that measured point (*depth* $= (n+1)l/2$, where $n = 1, 2, 3$ etc.). To performed it, the following procedure is carried out: a fixed position of AB current emission electrodes is kept, and a series of measurements is made by moving MN potential electrodes along measured profile with displacement equal to ℓ: $M_1N_1(n=1)$; $M_2N_2(n=2)$; $M_3N_3(n=3)$, and so on.

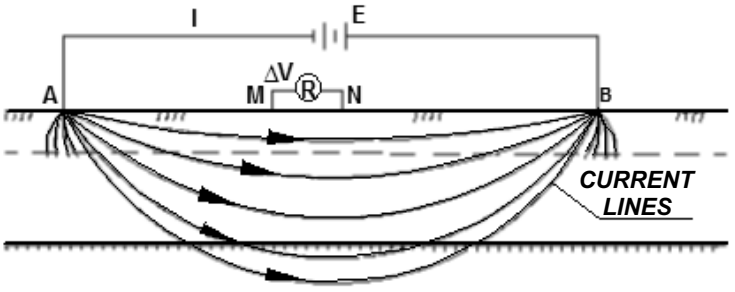

Figure 2 – Principle of Electrical Resistivity Method.

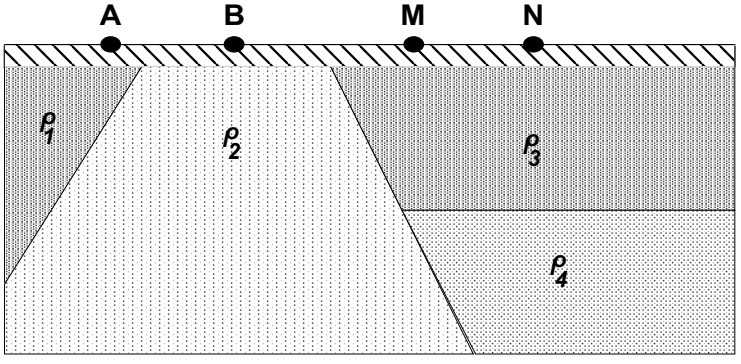

Figure 3 – Heterogeneous Substrate (Gallas, 2000, modified from Orellana, 1972).

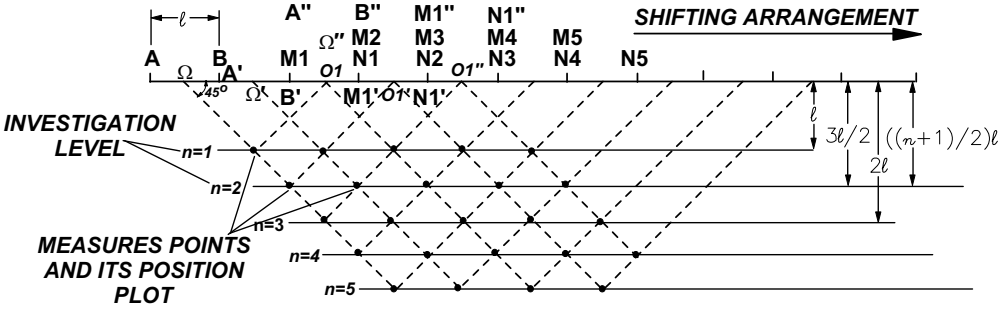

Figure 4 – IP-Resistivity Profiling/Disposition in dipole-dipole array field (Gallas, 2000).

In each station, two dipoles are displaced to a distance equal to ℓ, and obtained data are plotted in position $n = 1, 2, 3, \ldots$ and interpolated, generating an apparent IP-resistivity pseudosection.

At present, pseudosection results are processed in data inversion programs where modeled IP-resistivity sections are obtained. In theory, these sections reproduce, resistivity and chargeability (IP) distribution in subsurface (IP-Resistivity 2D model), more easily correlated to studied area geology.

This work presents IP and resistivity pseudosections as well as modeled sections of these parameters obtained by RES2DINV inversion program by Geotomo Software.

Gradient Array

In this array, also known as rectangle, the survey is developed in keeping AB current electrodes fixed with a gap equal to L, and performing readings through M and N potential electrodes that are displaced in lines parallel to *alignment* formed by A and B electrodes. MNs displacement amplitude is generally equal to l. The gap between M and N depends on the desired detail degree. L/l ratio usually is between 10 and 50. Figure 5 shows basic gradient device configuration.

Rectangle array research depth increases with L gap increment. Expecting electric field remains reasonably uniform

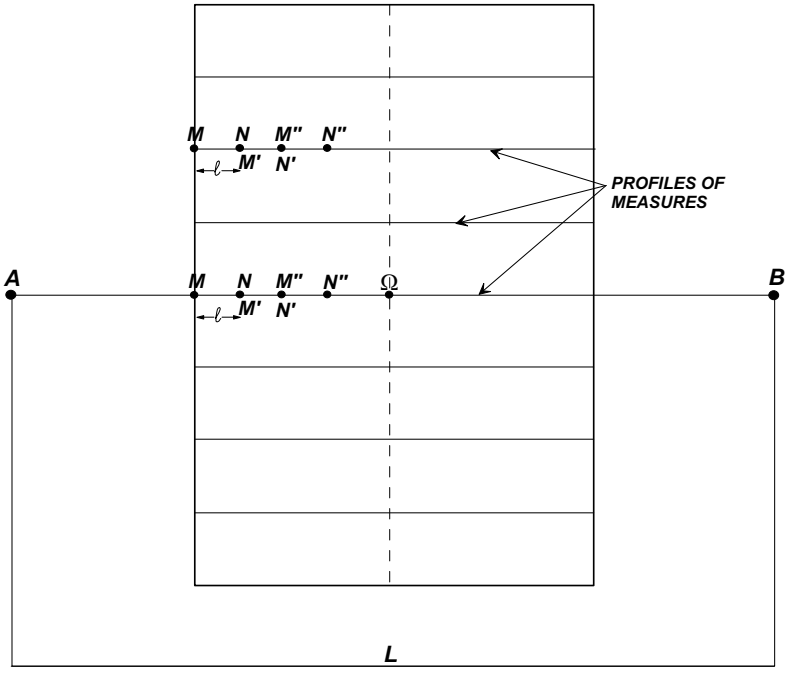

Figure 5 – Gradient or Rectangle Array (Gallas, 2000).

– approximately constant research depth –, measured points should be within a rectangle centered at Ω and AB midpoint, and its sides have the following dimensions:

– Lower side parallel to AB: approximately $L/3$;

– Higher side perpendicular to AB: approximately $L/2$.

The same equation presented in apparent resistivity item is used to calculate the apparent resistivity, and geometric K factor changes in each measurement station.

Simple computer program elaboration is not difficult for Ks calculation or tables and graphs with K values for L/l, and the midpoint coordinates between M and N (or AM, BM, AN and BN distances). K values for a single rectangle quadrant are calculated, and the other three quadrants are identical by symmetry.

FIELD SURVEYS

IP-resistivity geophysical surveys were carried out by using electrical profiling with gradient and dipole-dipole arrays. IP measurements were less effective than resistivity.

Two gradient arrays with $AB = 400$ m and $MN = 10$ m were carried out, covering 340 $\times$ 80 m area, totaling 25,600 m^2. Surveyed profiles, denominated lines A, B, C, D, E, F, G, H, and I were extended from –20 m to 320 m stakes. Lines were spaced 10 m from each other, and measurements also taken every 10 m. For quality control, an overlap ("clutch area") of measurements of 4 points on each line on both gradient arrays, was carried out, with repeated measurements from 140 to 180 m (Fig. 6).

The values adopted for the "clutch", for construction of complete map were those from gradient array 2. This was a choice among the 03 possible as could have been used the gradient 1 data or an average of both, with similar results.

In addition, after gradient survey, a D Line was chosen for a dipole-dipole detailing with $AB = MN = 10$ m, and 5 research levels. This line extension was from 20 m to 240 m stakes, totaling 220 m linear.

ANALYSIS OF RESULTS

Obtained results in this work are presented in the listed figures as following:

Figure 6 – Gradients 1 and 2, and "clutch" area.
Figure 7 – Map of gradient array resistivity.
Figure 8 – Map of gradient array chargeability (IP).
Figure 9 – Modeled resistivity pseudosection and section, D Line.
Figure 10 – Modeled IP pseudosection and section, D Line.

Figure 7 presents the overlap of the two gradient arrays with an AB gap of 400 m, measured every 10 m, grouped into a single map, composed by a total of 9 lines, 340 m long each, extending from –20 m to 320 m stakes.

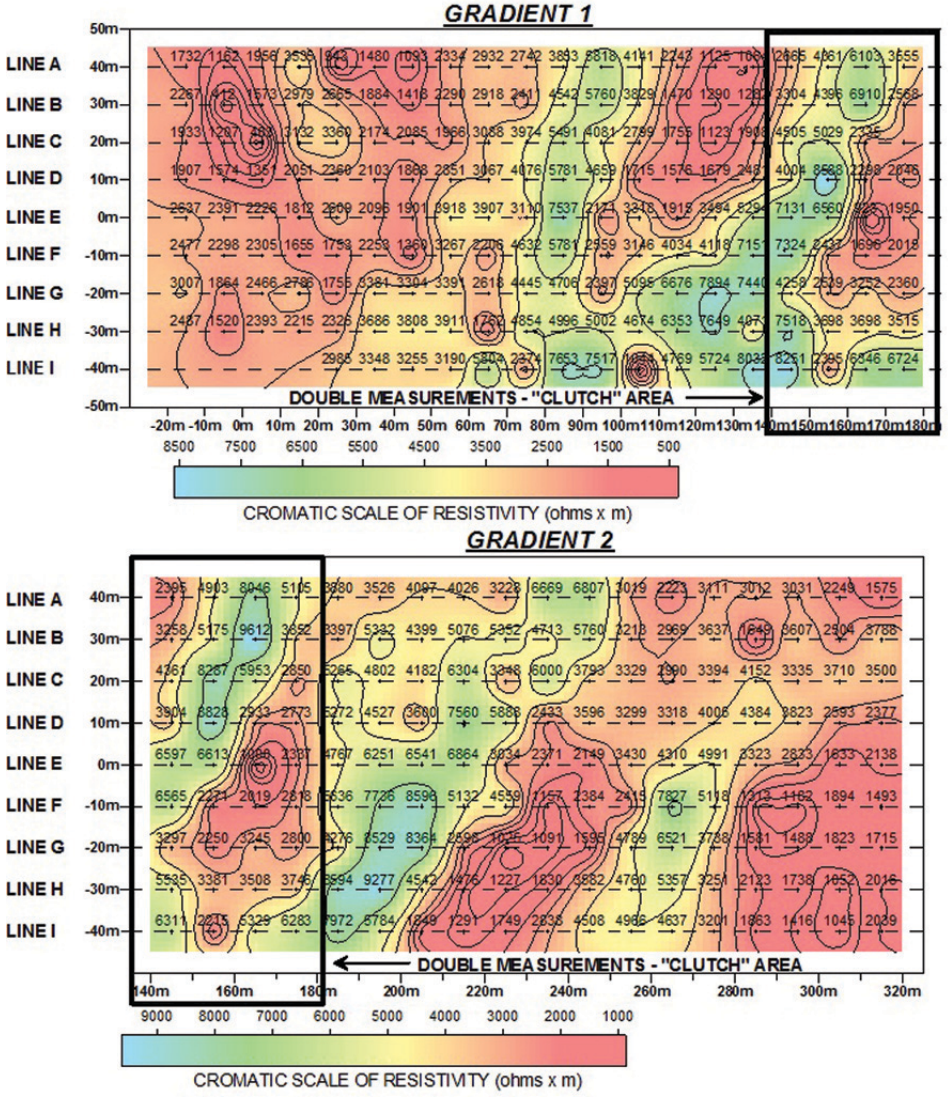

Figure 6 – Gradients 1 and 2, and "clutch" area.

The resistivity pattern observed in Figure 7 characterizes the NE-SW geological trend direction, forming an angle lesser than 20° with the surveyed lines direction.

Figure 8 presents a map with chargeability (IP) results showing a similar distribution as that observed for resistivity. However, there is a better visual definition in Figure 7.

Two resistivity patterns can be identified: the first of comparatively less high resistivity, below 2,000 Ω.m, and other relatively higher, above 5,000 Ω.m.

The use of IP-Resistivity for sulphide prospecting and environmental studies is common in the geophysical literature, however, the application of this method to quartz prospecting, used in this study, is unprecedent.

Theoretically, quartz veins should have higher resistivity such as those ones above 5,000 Ω.m. Otherwise, the induced polarization (IP) response related to quartz masses is unexpected, and cannot have a defined premise of high or low chargeability.

However, it is worth remembering that these quartz occurrences are probably from hydrothermal processes that alter the host rocks, and consequently they can give rise to lower resistivity. In this case they could be correlated to the lowest resistivity values.

After the survey with gradient array and their result analysis, D Line was chosen for a detailed dipole-dipole profile to quantitatively evaluate the depths of more/less resistive features detected, as well as IP data. Results obtained with this test are presented

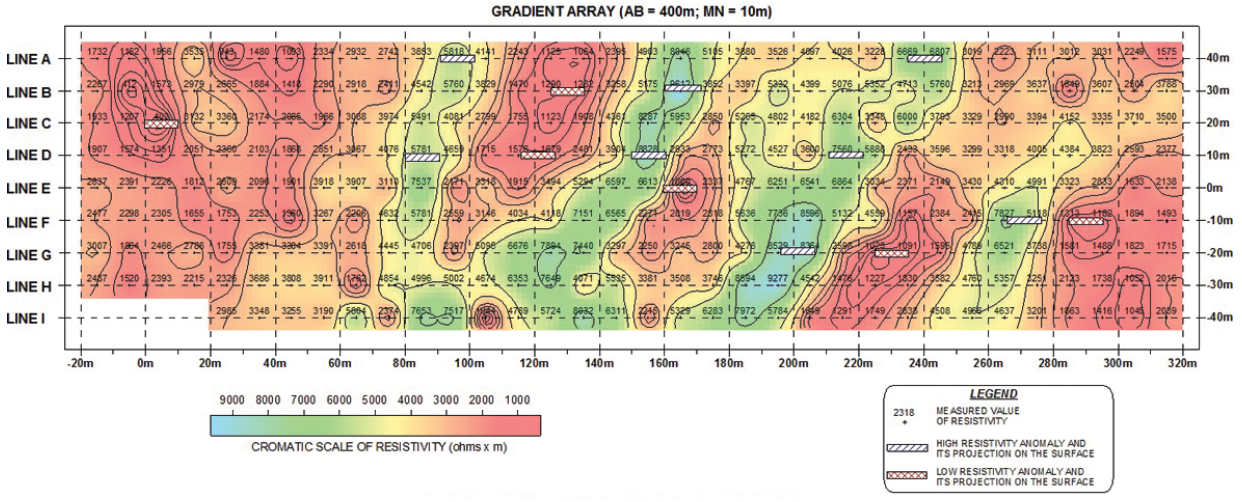

Figure 7 – Map of resistivity, gradient 1 + gradient 2.

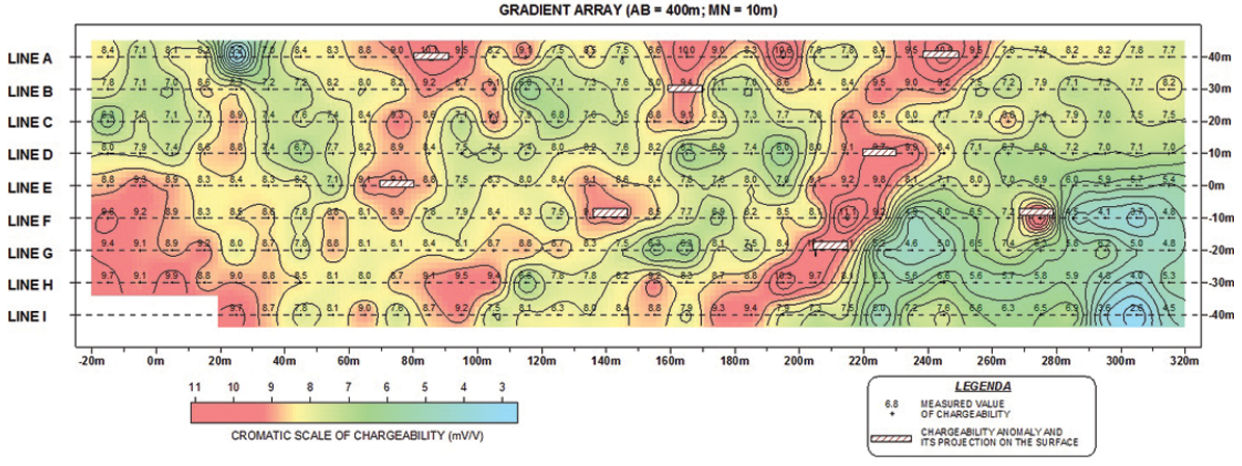

Figure 8 – Map of chargeability (IP), gradient 1 + gradient 2.

in Figures 9 and 10 as modeled resistivity and IP pseudosections and sections, in this order.

The D Line was chosen because it is located on the central area and intercepts the best resistivity and IP contrasts of identified "trends".

Modeled Pseudosections and Sections

Dipole-dipole IP-resistivity measurements were originally presented and interpolated (isovalue contours) only as pseudosections (Hallof, 1957) giving a visual representation of resistivity and chargeability behavior in subsurface. However, contour shapes do not depend solely on these measured distributions but also employed electrode configuration geometry. Even simple geometric shape (rectangular, for instance) bodies present completely different pseudosections in response to the used array (dipole-dipole, pole-dipole, pole-pole).

Accordingly, to obtain an IP-section more precise resistivity, it is necessary to implement the inversion process to the data which would theoretically lead to a reasonable approximation model for various geological structures (Gallas et al., 2011).

These inversion processes were used in the treatment of the survey dipole-dipole data by using the software RES2DINV by ABEM Instruments (ABEM, 1998), based on the algorithm developed by Loke & Barker (1996a, 1996b), whose investigation depths (software default) are according to Edwards (1977) proposal, and also they are about half estimated (Hallof, 1957) but they can be modified by software user.

Gallas & Verma (2006) and Gallas (1990) address the investigation depth issue, among other variables (dip, polarizable

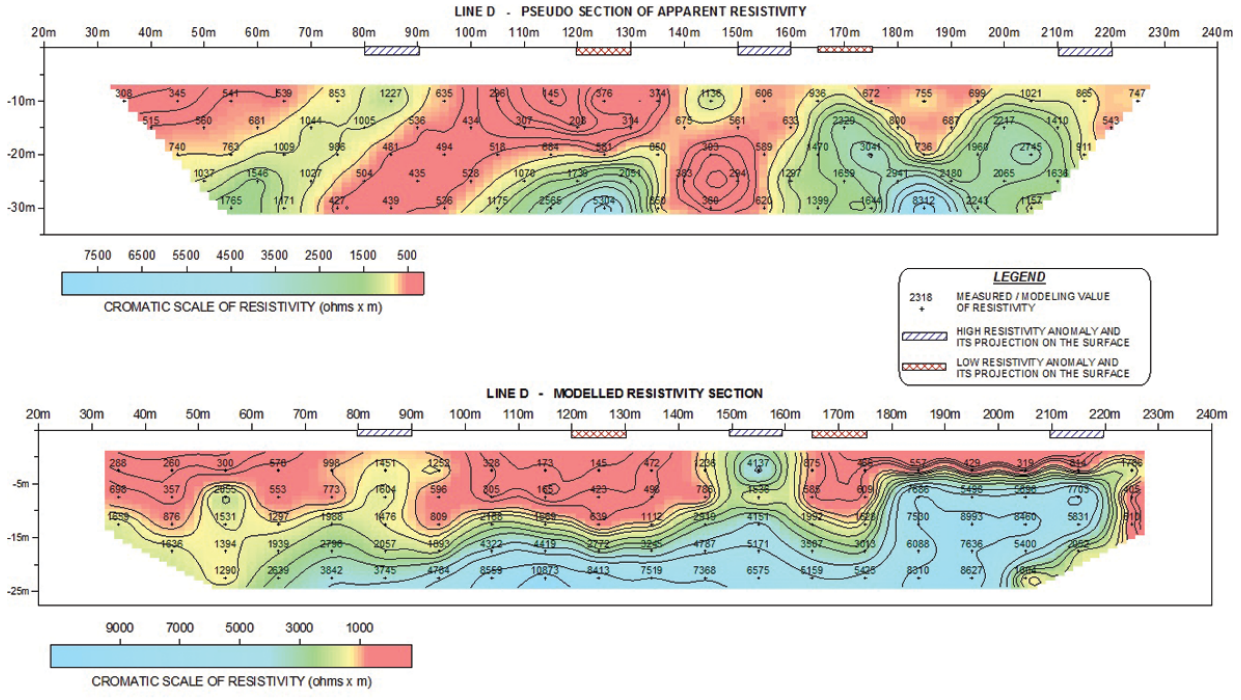

Figure 9 – Modeled resistivity pseudosection and section, D Line.

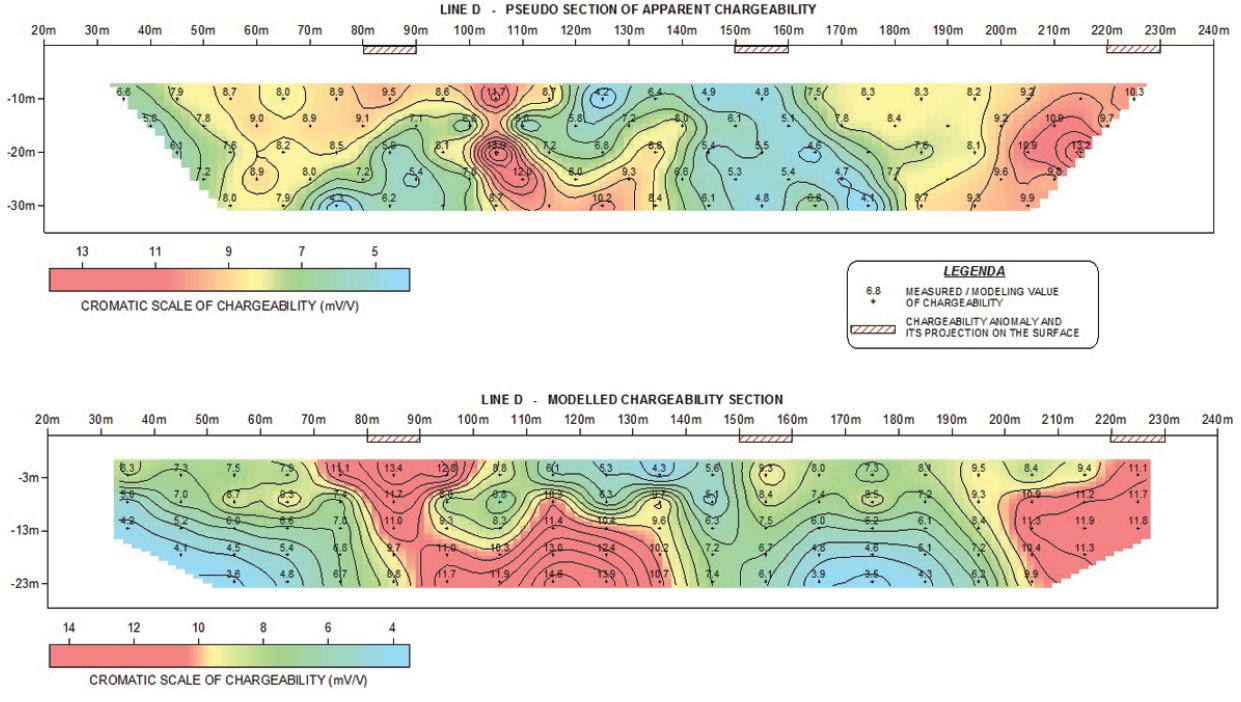

Figure 10 – Modeled chargeability pseudosection and section, D Line.

material content, thickness, etc.) by using cylindrical and tabular physical models for IP-resistivity analogical modeling in laboratory. Gallas (2003) suggests minimal dipole gaps based on expected depth where prospecting targets – fault/fractured areas under change coverage, in that case – are found.

Modeled sections are resulting from an automatic 2D inversion process. Resistivity data inversion processes seek to establish a probable real distribution model of IP-resistivity values in subsurface. Any distortions in pseudosections inherent to electrode arrays are theoretically eliminated by inversion processes.

Gradient Array

Regarding the gradient array – the main interest in this work – obtained data were not submitted to modeling/inversion processes, as in dipole-dipole. Used software does not include this electrode device, the electrode array has only a single research in-depth level and the program makes the two dimension inversion process.

Edwards (1977) uses empirical coefficients for penetration depths for dipole-dipole array, defining "effective research depth", also applied to other arrays, as gradient.

In Table 1, $L =$ gap between extreme array electrodes; $a =$ gap between (potential) measure electrodes, and $x =$ distance between the potential electrode center and the closest current electrode ($L/3 < x < L/2$).

Table 1 – Researched depths for gradient, according to Edwards (1977).

Gradient	Investigation
$L = 40$ a; $x = 20$ a	0.192L
$L = 40$ a; $x = 15$ a	0.163L
$L = 40$ a; $x = 10$ a	0.103L

Generally, for all practical purposes, the depth investigation by the gradient is estimated between 0 to 10%, and 0 to 25% of L (or AB), remembering measures correspond to the entire package located on referred intervals. Maximum and minimum penetration values depend on resistivity (and IP) of subjacent geoelectrical package.

A correlation between areas of higher resistivity and areas in which occur quartz masses (known as high resistivity) can be established as already mentioned. Moreover, the possible hydrothermal processes that originated these quartz masses may alter host rocks and provide lower resistivity to quartz mass/host rock set. Then, the two situations must be considered as potentially favorable to quartz mass occurrences.

As seen in Figures 9 and 10, projections in the surface of high/low resistivity regions as well as high chargeability are highlighted by a hatched bar. This standard is represented in section/pseudosection through blue-green and reddish yellow colors for high and low resistivity, in that order. For high chargeability, the corresponding color is reddish yellow.

In the gradient array resistivity map and in the modeled dipole-dipole pseudosection/section, the positions of points considered anomalous as well as high and low resistivity were indicated, and they should be considered in future direct researches, like digging and/or drillings.

Regarding chargeability (IP) data, detected anomalies were indicated in Figure 8, in modeled pseudosection and section (Fig. 10), and they must also be considered in future direct researches.

CONCLUSIONS

The geophysical surveys carried out in this study identified the most likely locations of the quartz mass occurrences. The method, however, cannot discern between neither hyaline nor quartz with rutile inclusions.

However, it should be reiterated that a direct detection of quartz with rutile and/or hyaline quartz, which are economically attractive, was not expected. Geophysical indications will specify favorable locations to quartz mass occurrences, regardless their quality.

Three main potential targets were identified: areas with high resistivity related to large massive quartz occurrences; areas of low resistivity related to hydrothermal quartz masses and areas of large chargeability IP anomalies related to massive quartz occurrences.

In the research aftermath, some of these targets were checked with trenches and wells, evidencing the occurrence of quartz masses corresponding to the lowest resistivity values.

The highest resistivity anomalies correspond to non-fractured granites, avoid of quartz masses.

Regarding IP, although it does not define anomalies as clear as resistivity, it indicated some correlation with the lowest chargeability values.

Thus, it can be seen that, at least for this type of prospecting, IP did not get results as satisfactory as Resistivity. Somehow, it was expected, since IP phenomenon manifests more strongly in the presence of disseminated sulphides and also of some clays. As seen in the field, both milky quartz masses and, even, hyaline or rutile quartz, sulphides and/or associated clays were not seen.

REFERENCES

ABEM INSTRUMENTS. 1998. Geoelectrical Imaging 2D & 3D – RES2DINV, ver. 3.3 for Windows 3.1, 95 and NT. Rapid 2D Resistivity & IP inversion using the least-squares method. By LOKE MH. ABEM Instruments, P.O. Box 20086, S-161 02 Bromma, Sweden.

BERTIN J & LOEB J. 1976. Experimental and theoretical aspects of induced polarization. Gebruder Borntraeger, Berlin-Stutgart, Germany: Geopublicaton Associates, v. 1, 250 pp.

EDWARDS LS. 1977. A modified Pseudosection for resistivity and induced-polarization. Geophysics, 3: 78–95.

GALLAS JDF. 1990. Modelamento Analógico de Polarização Induzida para Corpos Cilíndricos e Tabulares. Belém, Master dissertation in Geophysics, Pós-Graduação em Geociências, Universidade Federal do Pará, Brazil. 121 pp.

GALLAS JDF. 2000. Principais Métodos Geoelétricos e suas Aplicações em Prospecção Mineral, Hidrogeologia, Geologia de Engenharia e Geologia Ambiental. Rio Claro. Ph.D. Thesis (Geociências e Meio Ambiente), Instituto de Geociências e Ciências Exatas, Universidade Estadual Paulista, Brazil. 174 pp.

GALLAS JDF. 2003. Prospecção de água subterrânea com o emprego de métodos indiretos. Revista do Instituto Geológico, 24: 43–51.

GALLAS JDF & VERMA OP. 2006. Resistividade e Polarização Induzida (IP) – Modelagem Analógica. Brazilian Journal of Geophysics, 24(1): 25–35.

GALLAS JDF, TAIOLI F & MALAGUTTI FILHO W. 2011. Induced polarization, resistivity, and self-potential: a case history of contamination evaluation due to landfill leakage. Environmental Earth Sciences, 63: 251-261. DOI: 10.1007/s12665-010-0696-y.

HALLOF PG. 1957. On the interpretation of resistivity and induced polarization measurements. Cambridge, MIT, Ph.D. Thesis.

LOKE MH & BARKER RD. 1996a. Rapid least-squares inversion of apparent resistivity Pseudosections by a quasi-Newton method. Geophysical Prospecting, 44: 131–152.

LOKE MH & BARKER RD. 1996b. Practical techniques for 3D resistivity surveys and data inversion. Geophysical Prospecting, 44: 499–523.

ORELLANA E. 1972. Prospeccion geoeletrica en corriente continua. Madrid: Paraninfo, 523 pp.

SUMNER JS. 1976. Principles of induced polarization for geophysical exploration. New York: Elsevier Scientific Publishing Co., 277 pp.

Recebido em 30 junho, 2015 / Aceito em 25 maio, 2016
Received on June 30, 2015 / Accepted on May 25, 2016

NOTES ABOUT THE AUTHOR

José Domingos Faraco Gallas is B.Sc. in Geology from Universidade Federal do Rio Grande do Sul (UFRGS, 1978), M.Sc. in Geophysics from Universidade Federal do Pará (UFPA, 1990) and Ph.D. in Geosciences and Environment (focusing on Applied Geophysics) from Universidade Estadual Paulista (UNESP, 2000). Researcher at the Instituto de Pesquisas Tecnológicas (IPT – Institute for Technological Research of the São Paulo State, from 1979 to 2002). Professor of the Geosciences Institute of the Universidade de São Paulo (USP, since 2002). During a period of license from USP (2004-2005) was Adjunct Professor of the Universidade do Vale do Rio dos Sinos (Unisinos). Areas of research interest are applied geophysics to mineral exploration, hydrogeology, engineering geology and environmental geology.